



## Localized attack of copper and brass in tap water: the effect of *Pseudomonas*

M.B. Valcarce, S.R. de Sánchez, M. Vázquez \*

*División Corrosión, INTEMA, Facultad de Ingeniería, UNMdP,  
Juan B. Justo 4302, B7608FDQ Mar del Plata, Argentina*

Available online 13 August 2004

---

### Abstract

The presence of *Pseudomonas fluorescens* in artificial tap water (ATW) affects the composition of the oxide layer and the susceptibility to pitting corrosion of copper and 70/30 brass. The surface layer was investigated by means of a combination of electrochemical and spectro-electrochemical techniques involving cyclic voltammograms, potentiodynamic reduction curves, anodic polarisation curves, weight-loss tests and reflectance spectroscopy.

In the sterile conditions the mass loss is lower in brass than in copper while the presence of bacteria enhances the attack in brass. Dezincification in inoculated electrolyte was revealed by microscopic observation, as well as by potentiodynamic reduction curves. Zn dissolution was also supported by spectroscopic evidence.

Slow-rate voltamperometric curves were used to determine potential values characteristic of localized corrosion. In the presence of bacteria, the pitting potential moves towards more positive values for both materials but the difference between the repassivation and the pitting potential increases. Bigger and deeper pits can be seen in the presence of microorganisms.

© 2004 Elsevier Ltd. All rights reserved.

*Keywords:* A. Copper; A. Brass; C. De-alloying; C. Microbiological corrosion; C. Passive films

---

---

\* Corresponding author. Tel.: +54 223 481 6600; fax: +54 223 481 0046.  
E-mail address: [mvazquez@fi.mdp.edu.ar](mailto:mvazquez@fi.mdp.edu.ar) (M. Vázquez).

## 1. Introduction

Copper and its alloys belong to the group of materials that are resistant to corrosion thanks to a protective film that grows naturally in certain environments. One of the most frequent problems that appears on copper and copper-alloys is microbiologically induced corrosion (MIC), which can be attributed to the presence of bacteria that changes the condition in the metal/electrolyte interface and promote localized corrosion. The mechanism typical of this kind of attack has been studied in carbon steels [1,2], where the phenomenon is well understood particularly for the case of sulphate-reducing bacteria. This interest has also expanded to other materials such as stainless steels [3,4] and copper-alloys [5–7], which are generally resistant to corrosion. These materials are susceptible to MIC in the conditions mentioned above for carbon steels, as well as in other aqueous aerobic media where different mechanisms have been proposed to explain the potential ennoblement leading to pitting. Among these proposed mechanisms, the production of enzymes that catalyse oxygen reduction [8] or the effect of other metabolites on the metal surface [6,9,10] are worth mentioning. All of them share a common pattern: the important role of the surface film and the changes induced by the presence of bacteria [7].

Copper and brass are materials of widespread use for plumbing purposes. The presence of organic matter is known to have undesirable effects in the quality of the drinking water. This can be manifested by either increasing corrosion by-products release or by decreasing microbial stability [11]. Moreover, potable water installations have frequently found to be affected by pitting of the piping system. In many of these cases, microbiologically influenced corrosion has been found to be the origin of the problem. This investigation describes the study of the first stages of microbiological attack by means of a combination of electrochemical and spectroscopic techniques.

## 2. Materials and methods

### 2.1. Electrolyte composition

All the experiments were carried out using artificial tap water (ATW). The mineral base composition was  $\text{MgSO}_4$  ( $40 \text{ mg l}^{-1}$ ),  $\text{MgCl}_2$  ( $60 \text{ mg l}^{-1}$ ),  $\text{KNO}_3$  ( $25 \text{ mg l}^{-1}$ ),  $\text{CaCl}_2$  ( $110 \text{ mg l}^{-1}$ ),  $\text{Na}_2\text{CO}_3$  ( $560 \text{ mg l}^{-1}$ ) and  $\text{NaNO}_3$  ( $20 \text{ mg l}^{-1}$ ) in distilled water; the pH was adjusted to 7.6 with HCl solution  $1 \text{ mol l}^{-1}$ .

In the case of the electrochemical and spectroelectrochemical tests performed to evaluate the effect of the presence of bacteria, pure cultures of *Pseudomonas fluorescens* (ATCC 17552) were grown at  $32 \text{ }^\circ\text{C}$  with continuous shaking in a minimal broth containing 0.06% peptone. Cells were harvested from cultures at the mid-exponential phase of growth by centrifugation for 10 min at  $10,000g$  in a Jouan BR4i centrifuge, washed, and suspended in ATW after centrifuging again. This bacterial suspension was labelled as “BATW”.

The weight loss tests were done in ATW containing 0.5% peptone.

## 2.2. Metal samples preparation

Disc samples of aluminium brass (Al-brass, UNS 68700) and copper were included in fast curing acrylic resin on appropriated PVC holders with an electric contact at the back. Samples were abraded to grade 600 with emery paper, and mirror polished with 0.05  $\mu\text{m}$  alumina powder (Type B–Buehler, Lake Bluff, USA). After that, samples were rinsed gently with distilled water. The geometrical area exposed was 0.312  $\text{cm}^2$  in the case of copper and 0.554  $\text{cm}^2$  for brass.

In the case of weight loss tests, aluminium brass and copper coupons were abraded only up to grade 600 with emery paper. The exposed area was 12  $\text{cm}^2$ .

## 2.3. Electrochemical measurements

A three-electrode electrochemical cell was used. A saturated calomel electrode (SCE,  $E = 0.24$  V vs. NHE) was used as reference and a platinum wire of large area as counter electrode.

The electrochemical instrumentation included a Voltalab PGP 201 potentiostat and a Solartron SI 1280B unit.

When cyclic voltammograms were recorded, the electrolyte was deaerated 15 min with  $\text{N}_2$  prior to each measurement. The electrodes were then pretreated by holding them at  $-1.1$  V for 5 min in ATW. Finally the scan was started at  $-1.1$  V which was reversed at a convenient potential. The sweep rate was 10  $\text{mVs}^{-1}$ .

To carry out potentiodynamic reductions, the electrodes were prerduced in ATW at  $-1.1$  V for 15 min to obtain a reproducible, clean surface. After that, the passive film was grown on the metallic surfaces at a desired potential for a given time. Then the electrode was immediately transferred to another cell where the oxides were reduced in deaerated electrolyte applying a potentiodynamic scan at a rate of 10  $\text{mVs}^{-1}$ . The starting point was the positive potential where the oxide had been grown. The potential was scanned in the negative direction up to  $-1.1$  V.

When anodic polarisation curves were registered, the electrodes were first pretreated in ATW at  $-1.1$  V for 15 min. Subsequently, they were left at open circuit potential ( $E_{\text{corr}}$ ) for 2 h. The passive layer was then stable. Finally a potentiodynamic scan was started at the corrosion potential, using a sweep rate of 10  $\text{mVs}^{-1}$ . The scan direction was reversed at  $2.18 \times 10^{-4}$   $\text{A cm}^{-2}$  in the case of brass and at  $6.40 \times 10^{-4}$   $\text{A cm}^{-2}$  in the case of copper. These values were chosen to induce a convenient degree of attack. The overall procedure follows the recommendations of ASTM [12].

## 2.4. UV–visible reflectance spectroscopy

The spectroelectrochemical measurements were carried out using a commercial double-beam spectrophotometer (Shimadzu UV 160A) conveniently modified as described elsewhere [13,14]. Surface oxides were potentiostatically grown on aluminium brass and copper in the sample compartment. Chosen potentials and times

are indicated where relevant. The absorption spectra were then recorded in situ. Baseline corrections were carried out by polarising two identical polished surfaces at  $-1.1$  V to prevent oxide growth.

To evaluate the effect of the presence of bacteria on the surface films, the electrolyte was replaced by BATW after recording the baseline. The electrodes were then kept at open circuit potential for 2 h. To avoid interference in the absorption signal, the solution was replaced again with sterile ATW prior to recording the reflectance spectra.

### 2.5. Weight loss determinations

Previously weighted coupons were suspended and immersed in the test solution, arranging three coupons in each of four containers. The containers were then sterilized for 20 min at  $120$  °C. Two of them, one with copper and one with aluminium brass, were kept sterile and left as reference while the other two containers were inoculated with bacteria (culture). The containers were kept at  $32$  °C with gentle agitation. Every seven days, 1 ml of ATW containing 0.5 g of peptone was added in sterile conditions.

The coupons were withdrawn after 90 days and the corrosion products were stripped by immersion in HCl 10%. Then they were neutralised and rinsed, first with saturated  $\text{Na}_2\text{CO}_3$  solution, and finally with distilled water. The cleaned and dried coupons were weighted and observed with a metallographic microscope.

The copper and zinc concentrations in the test solutions were evaluated by atomic absorption spectrophotometry [15]. To do so, the solutions were acidified to pH 1 with concentrated HCl and the biomass was then harvested by centrifugation at  $10,000g$  with a Jouan BR4i centrifuge.

## 3. Results and discussion

### 3.1. Characterisation of the surfaces by cyclic voltammetry

Fig. 1 shows the cyclic voltammogram of copper and brass in contact with deaerated artificial tap water (ATW). In the case of copper, oxide growth starts at potentials positive to  $-0.33$  V. A sharp anodic peak (Ia) is evident at  $-0.2$  V and localized corrosion initiates at potentials positive to  $0.05$  V. By changing the amplitude of the potential window and by comparison with results obtained using  $0.1 \text{ mol l}^{-1}$  borax as electrolyte [16,17], peak Ia can be attributed to the formation of Cu(I) species. In a similar way, the cathodic peak Ic at  $-0.11$  V can be assigned to the reduction of Cu(II) species while peak IIc at  $-0.49$  V can be attributed to the reduction of those Cu(I) species formed in association with peak Ia. The absence of a second anodic peak and the appearance of a third cathodic peak (IIIc) just at the beginning of the hydrogen evolution region have been found before by other authors [18]. The third cathodic peak could be attributed to the desorption or reduction of an adsorbed submonolayer. Both features are found to be very dependent on the

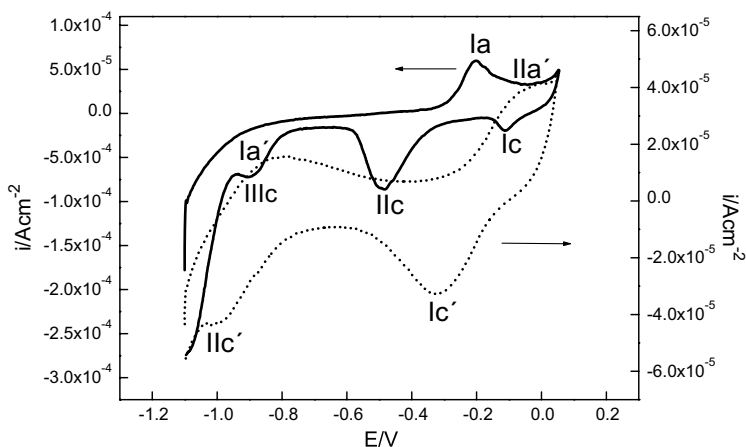


Fig. 1. Cyclic voltammograms of copper (—) and brass (---) in ATW. Scan rate: 10 mV s<sup>-1</sup>.

positive limit of the potential sweep and on the concentration of certain anions in the electrolyte.

In the case of brass, the cyclic voltammogram shows an anodic peak Ia' at -0.80 V and a shoulder (IIa') for potentials higher than -0.25 V. At 0.05 V localized corrosion appears. Cathodic peak Ic' can be attributed to the reduction of cuprous compounds, while peak IIc' appears to be related to the reduction of Zn(II) species [16,17].

### 3.2. Characterisation of the surfaces by reflectance spectroscopy

The composition of the oxide layer on copper was further studied by potentiostatic growth of a film at the potential of the anodic peak in Fig. 1. The film was subsequently characterised by reflectance spectroscopy and potentiodynamic reduction. Fig. 2 presents the reflectance spectrum typical of a copper electrode held at -0.20 V for 15 min. The absorbance peaks at 550 and 380 nm are characteristic of Cu<sub>2</sub>O [13,14,19]. When the film is potentiodynamically reduced, two cathodic peaks appear (see Fig. 3), in good agreement with those found in the voltammogram shown in Fig. 1. A new spectrum recorded after the potential scan, confirms complete reduction. A similar result can be found if the anodic film is grown at more positive potentials, although the reduction peaks slightly move in the negative direction. On the other hand, when copper is held at -0.30 V, no oxide growth can be revealed by reflectance spectroscopy (see Fig. 2) instead, when recording the *i*-*V* curve, a shoulder in the vicinity of the potential of peak IIIc in Fig. 1 is still present (Fig. 3).

An equivalent experimental sequence was performed on brass. The corresponding results are presented in Figs. 4 and 5. When the anodic film is formed at -0.1 V, the reflectance spectra shows a shoulder at 460 nm which can be taken as evidence of

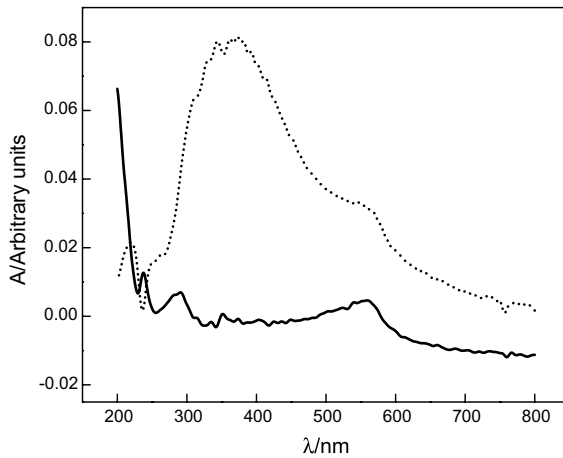


Fig. 2. Reflectance spectra for oxides grown on copper at  $-0.2$  V (---) and  $-0.3$  V (—) for 15 min in ATW.

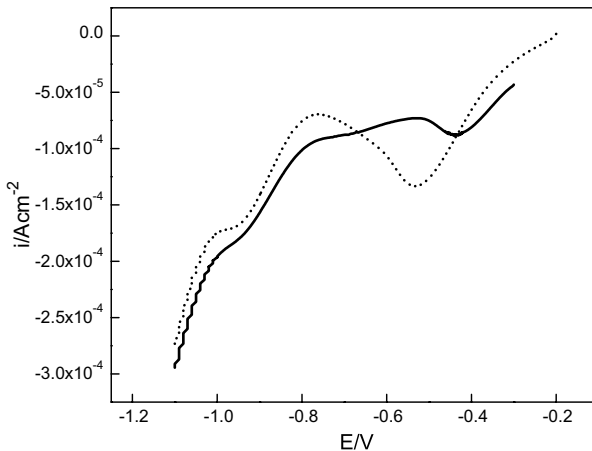


Fig. 3. Potentiodynamic reduction curves for oxides grown on copper at  $-0.2$  V (---) and  $-0.3$  V (—) for 15 min in ATW. Scan rate:  $10 \text{ mV s}^{-1}$ . Scan starts at growth potential.

$\text{Cu}_2\text{O}$  and also a peak at 260 nm characteristic of the participation of Zn(II) species in the film structure [19,20] (see Fig. 4). When the film is potentiodynamically reduced, two cathodic peaks appear at  $-0.57$  and  $-0.83$  V respectively (Fig. 5), again in good agreement with those in the cyclic voltammogram (Fig. 1). When the film is grown at more negative potentials, the main features of the spectrum are still evident at potentials as negative as  $-0.80$  V (Fig. 4). However upon reduction, the current decreases markedly (Fig. 5). The presence of  $\text{Cu}_2\text{O}$  at  $-0.8$  V could be related to the selective dissolution of Zn at potentials negative to  $-0.50$  V. As suggested before

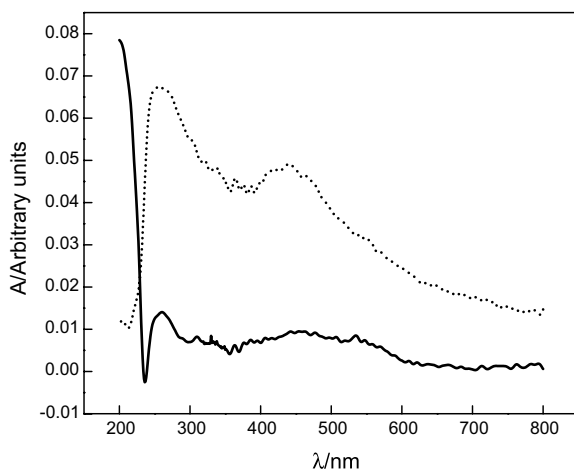


Fig. 4. Reflectance spectra for oxides grown on brass at  $-0.1$  V (---) and  $-0.8$  V (—) for 60 min in ATW.

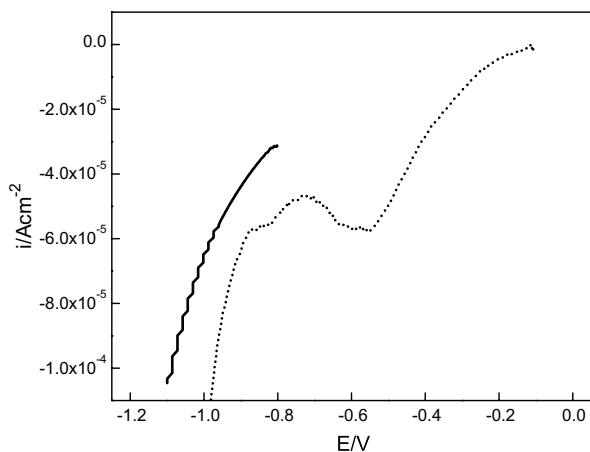


Fig. 5. Potentiodynamic reduction curves for oxides grown on brass at  $-0.1$  V (---) and  $-0.8$  V (—) for 60 min in ATW. Scan rate:  $10 \text{ mV s}^{-1}$ . Scan starts at growth potential.

by other authors, dezincification might induce the formation of copper oxides at potentials that are more negative than those found for pure copper [16].

### 3.3. Surface films formed at open circuit potential: the effect of the presence of bacteria in the electrolyte

The effect of the presence of bacteria on the composition of the surface films formed at open circuit potentials was also investigated. Potentiodynamic reduction

curves of copper and brass electrodes kept for 120 min at open circuit potential are compared in Fig. 6. Both curves show characteristic features typical of those described above for anodically grown films. On copper, the presence of bacteria while the surface layer is growing seems to have no notable effect on the potentiodynamic reduction curves. On the other hand, on brass the peak assigned to Cu(I) species shifts in the positive direction in the presence of bacteria during the film growth, while the peak ascribed to Zn(II) species is no longer evident (Fig. 7). This result suggests that the passive layer loses Zn(II) when formed in the presence of bacteria in the electrolyte.

Reflectance spectra recorded for brass surfaces that have been exposed to bacteria confirm dezincification. Fig. 8 compares the spectra of brass held for 2 h at the corrosion potential in contact with ATW with and without bacteria. When the surface layer has been formed in contact with bacteria, a broad peak can be seen between 330 and 480 nm. This has been attributed before by other authors [21] to a surface layer enriched in copper. Also, the relative intensity of the Zn(II) peak at 260 nm clearly decreases, in agreement with the selective dissolution of Zn from the passive layer that has been proposed above. In the case of copper, no differences could be found between the reflectance spectra obtained when bacteria are present in the electrolyte while the electrode is kept at open circuit potential.

### 3.4. Weight-loss tests

Table 1 presents the weight-loss results for copper and brass after ninety days exposure to inoculated (culture) and sterile (blank) ATW. As for copper, pitting was only evident in those specimens in contact with the culture, where in general,

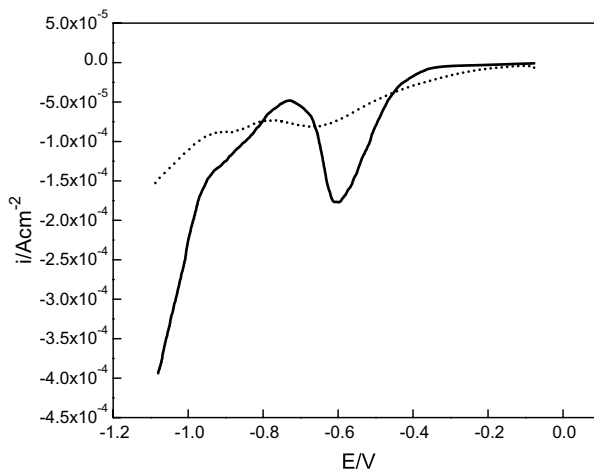


Fig. 6. Potentiodynamic reduction curves for oxides grown on copper (—) and brass (---) at the corrosion potential for 120 min in ATW. Scan rate:  $10 \text{ mV s}^{-1}$ . Scan starts at open circuit potential.



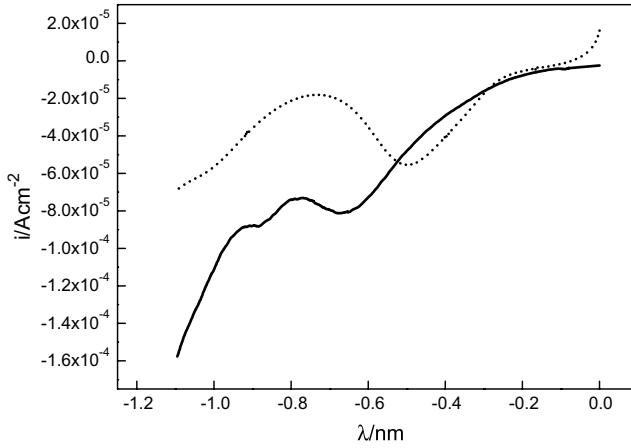


Fig. 7. Potentiodynamic reduction curves for oxides grown on brass at the corrosion potential for 120 min in sterile ATW (—) and BATW (---). Scan rate: 10 mVs<sup>-1</sup>. Scan starts at open circuit potential.

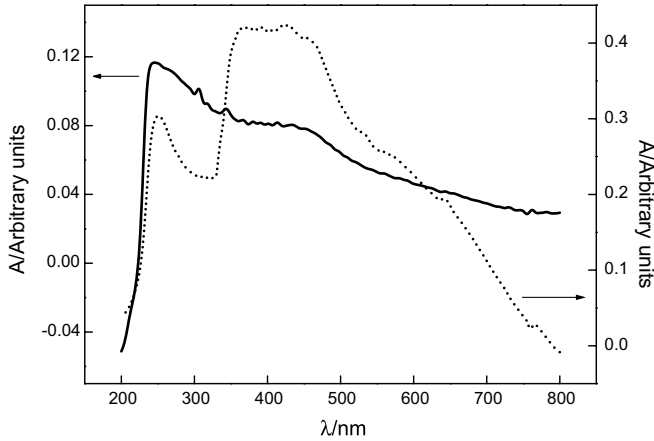


Fig. 8. Reflectance spectra for oxides grown on brass at the corrosion potential for 120 min in sterile ATW (—) and BATW (---).

Table 1

Weight-loss results for copper and brass after a 90-days period in contact with sterile and inoculated ATW

	Cu + culture	Cu (blank)	Brass + culture	Brass (blank)
Weight loss (mgcm <sup>-2</sup> )	4.7	2.2	1.2	0.2
Type of attack	Pitting	None	Pitting and dezincification	Pitting

the surface also appeared to be rougher (see Fig. 9a and b). The mass lost in the presence of bacteria increased by a factor of 2.4.

In the case of brass coupons, pitting could be observed both in presence of bacteria and in sterile electrolyte (see Fig. 9c and d). When observed under the microscope, the surfaces in contact with the culture appeared to be reddish in colour, which could be associated to copper enrichment in the film. When weight-loss results are analysed (Table 1), it can be observed that in both exposure conditions mass loss is lower than in the case of copper. However, the presence of bacteria enhances dissolution by a factor of 6.7.

Copper and zinc contents in the solutions in contact with the coupons were analysed by atomic absorption spectroscopy. The results are summarised in Table 2. As

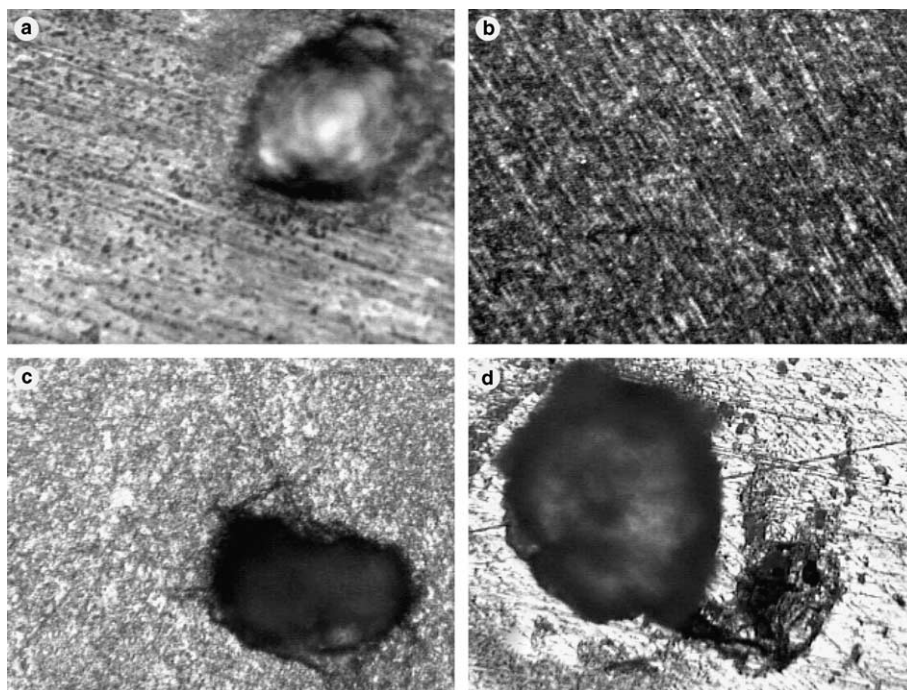


Fig. 9. Micrographs (20 $\times$ ) of coupons surface after 90 days of exposure. (a) Cu + culture, (b) Cu blank, (c) brass + culture and (d) brass blank.

Table 2

Cu and Zn masses determined by atomic absorption spectroscopy, in the solutions in contact with the coupons prepared for weight-loss evaluation

	Copper (mg)	Zinc (mg)
Culture	25.62	4.81
Blank	4.15	0.82

can be seen, dissolution increases by a factor of about 6 in the presence of bacteria, in good agreement with corrosion results evaluated by mass loss (see above).

Non-uniform corrosion attack observed after long exposure periods of time is typical of pits that initiate and develop beneath a layer of corrosion products [22], which in this case can even constitute a biofilm.

### 3.5. Localized corrosion: the effect of the presence of bacteria in the electrolyte

The influence of the presence of bacteria on some relevant electrochemical parameters associated to pitting was also investigated. The results obtained for typical anodic polarisation curves are presented in Figs. 10 and 11 for copper and brass respectively. Table 3 presents average values for the pitting potential ( $E_p$ ), repassivation potential ( $E_{rp}$ ) and corrosion potential ( $E_{corr}$ ), taking into account at least three independent experiments, for copper and brass in the two environments (sterile ATW and BATW). The direction of the potential sweep was reversed at predetermined current density values to make the visual comparison of the surfaces more significant. When observed at the microscope, copper surfaces presented more density of pits, which are also bigger and deeper when the samples are in contact with the bacterial suspension (see Fig. 12).

Comparing copper and brass in sterile ATW (Table 3), it can be seen that the presence of zinc as an alloying element moves the pitting potential towards less positive (noble) values. The difference ( $E_p - E_{corr}$ ) is also higher for copper. These facts are in good agreement with the results of weight-loss (Section 3.4), where copper showed no pitting while brass did. When copper and brass are compared under the effect of the presence of bacteria in the electrolyte, similar values are found for the differences between ( $E_p - E_{corr}$ ), ( $E_p - E_{rp}$ ) and ( $E_{rp} - E_{corr}$ ). This could be

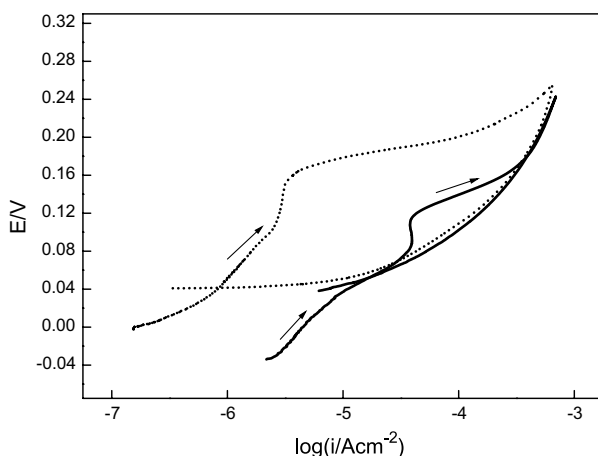


Fig. 10. Anodic polarisation curves of copper in sterile ATW (—) and BATW (---). Scan rate:  $10 \text{ mVs}^{-1}$ . Scan starts at open circuit potential.

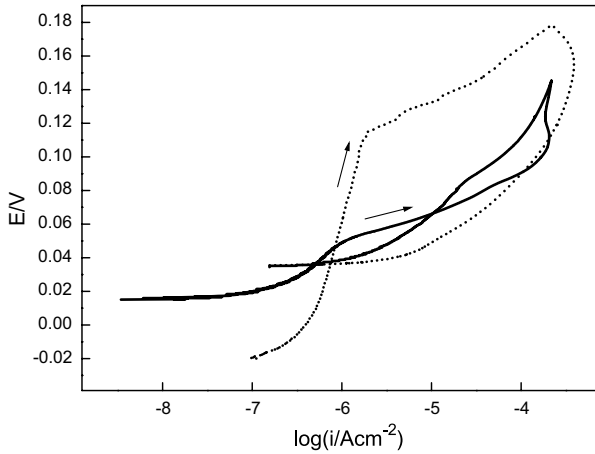


Fig. 11. Anodic polarisation curves of brass in sterile ATW (—) and BATW (---). Scan rate: 10 mVs<sup>-1</sup>. Scan starts at open circuit potential.

Table 3

Relevant electrochemical parameters that characterise the anodic polarisation curves in copper and brass

	Cu sterile ATW	Cu BATW	Brass sterile ATW	Brass BATW
$E_p$ (mV)	131 ± 18	150 ± 8	56 ± 13	127 ± 12
$E_{corr}$ (mV)	-31 ± 16	-10 ± 7	-1.5 ± 12	-32 ± 28
$E_p - E_{corr}$	162	160	57	160
$E_{rp}$ (mV) <sup>a</sup>	70 ± 28	42 ± 4	45 ± 16	31 ± 7
$E_p - E_{rp}$	61	109	11	96
$E_{rp} - E_{corr}$	101	51	47	63

<sup>a</sup> The scan direction was reversed at  $2.18 \times 10^{-4} \text{ A cm}^{-2}$  in the case of brass and at  $6.40 \times 10^{-4} \text{ A cm}^{-2}$  in the case of copper.

related to the preferential dissolution of Zn and the consequent Cu enrichment that has been discussed above for brass in the culture.

In the case of copper, no big difference could be found between pitting potentials and corrosion potentials with and without bacteria present in the electrolyte (Table 3). However, it is interesting to observe the difference between the repassivation potential and the corrosion potential ( $E_{rp} - E_{corr}$ ), where the value for copper in contact with the culture is much less favourable. This confirms the results presented in Fig. 12. Furthermore, from the forward half of the polarisation curve (Fig. 10), it can be seen that copper attains the  $6.40 \times 10^{-4} \text{ A cm}^{-2}$  where the scan direction is reverted approximately 900 s after  $E_p$  when bacteria are present in the electrolyte, while in the sterile solution 1300 s are necessary to reach the same current density value. It can then be argued that the presence of microorganisms accelerates the localised attack. Also, greater hysteresis is evident in the polarisation curve after reverting the scan in the presence of bacteria. This can be correlated to a difficult

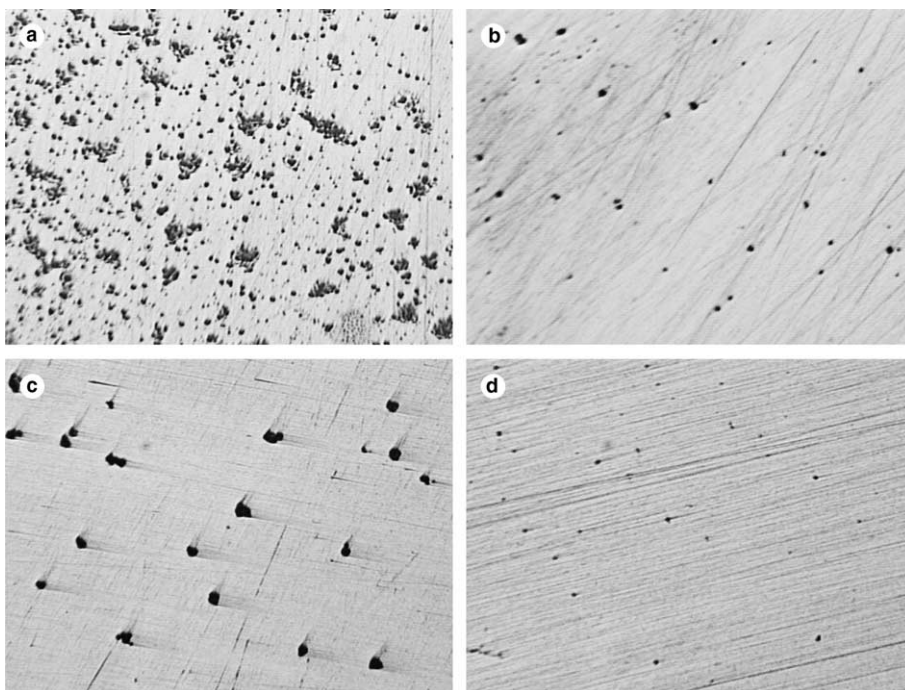


Fig. 12. Micrographs (5 $\times$ ) of electrode surface after performing anodic polarisation curves. (a) Cu + BATW, (b) Cu + sterile ATW, (c) brass + BATW and (d) brass + sterile ATW.

repassivation process, a situation where pits that initiated in the forward scan continue to grow easily.

When considering the situation for brass it can be seen that the values obtained for  $E_p$  and for the difference ( $E_p - E_{corr}$ ) are both more positive in the presence of the culture (Table 3). Simultaneously, the values for ( $E_p - E_{rp}$ ) in sterile ATW and BATW are also higher when bacteria are present in the electrolyte, which is consistent with a higher degree of corrosion (Fig. 12). Similarly to the situation for copper, brass takes 570 s from  $E_p$  to the  $2.18 \times 10^{-4} \text{ A cm}^{-2}$  where the scan direction is reverted in BATW while in the sterile ATW almost twice that time (940 s) is necessary to reach the same current density value. As for copper, also the hysteresis is greater in the presence of bacteria. Here again, the presence of bacteria through the production of certain metabolites seems to hinder repassivation.

#### 4. Conclusions

The anodic growth of surface films on copper and brass was investigated in artificial tap water. The effect of the presence of *Pseudomonas* was analysed by a combination of electrochemical and spectroscopic techniques. In the case of copper, the

oxide layer is mainly composed of cuprous oxide and the presence of bacteria has no particular effect on the composition of the surface film. In the case of brass, the incorporation of Zn(II) compounds to the surface film could be detected, together with its preferential dissolution upon reduction of the film in the presence of bacteria in the electrolyte.

Long term immersion tests show that localised corrosion (pitting) develops in brass, both in sterile and inoculated ATW, while for copper pits appear only in the presence of bacteria. From weight-loss evaluation it can be deduced that the total mass lost is greater in copper. However, in the presence of bacteria, dissolution increased by a factor of 7 in brass and just 2 in copper. The surfaces show clear visual evidence of dezincification in the presence of bacteria, in good agreement with the electrochemical results.

The electrochemical evaluation of localised corrosion shows that the pitting potential is more positive in the presence of bacteria, particularly for brass. However, repassivation is more difficult in BATW. Also, the time involved in reaching a given current density is less and the degree of attack is higher when microorganisms are present in the electrolyte.

The interpretation of fast response tests, such as polarisation curves, can be misleading when compared to corrosion experiments carried out over more extended periods of time [23] particularly when dealing with systems containing living microorganisms. A biofilm develops only over extended periods of time, creating regions of restricted flux where ions and metabolites can concentrate generating particularly aggressive local environments [24,25].

## Acknowledgements

This work has been supported by the National Research Council of Argentina (CONICET) and Third World Academy of Science (TWAS).

## References

- [1] G.A. Cragnolino, D.S. Dunn, P. Angell, Y.M. Pan, N. Sridhar, in: Corrosion 98 Conference, paper no. 147, NACE, 1998.
- [2] W.A. Hamilton, *Annu. Rev. Microbiol.* 39 (1985) 195.
- [3] J.E.G. Gonzalez, F.J.H. Santana, J.C. Mirza-Rosca, *Corros. Sci.* 40 (1998) 2141.
- [4] S.E. Werner, C.A. Johnson, N.J. Laycock, P.T. Wilson, B.J. Webster, *Corros. Sci.* 40 (1998) 465.
- [5] T.S. Rao, K.V.K. Nair, *Corros. Sci.* 40 (1998) 1821.
- [6] D. Wagner, A.H.L. Chamberlain, W.R. Fischer, J.N. Wardell, C.A.C. Sequeira, *Mater. Corros.* 48 (1997) 311.
- [7] J.T. Walker, K. Hanson, D. Caldwell, C.W. Keevil, *Biofouling* 12 (1998) 333.
- [8] V. Scotto, M.E. Lai, *Corros. Sci.* 40 (1998) 1007.
- [9] J.P. Busalmen, M. Vázquez, S.R. de Sánchez, *Electrochim. Acta* 47 (2002) 1857.
- [10] B.H. Olesen, R. Avci, Z. Lewandowsky, in: Corrosion 98 Conference, paper no. 275, NACE, 1998.
- [11] N. Boulay, M. Edwards, *Wat. Res.* 35 (2001) 683.
- [12] American Society of Testing and Materials, ASTM G 61-86, Philadelphia, 1993.

- [13] R.E. Hummel, *Physics State Solid (a)* 76 (11) (1983) 12.
- [14] S.R. de Sánchez, L.E.A. Berlouis, D.J. Schiffrin, *J. Electroanal. Chem.* 307 (1991) 73.
- [15] P. Ahuja, R. Gupta, R.K. Saxena, *Process Biochem.* 34 (1999) 77.
- [16] J. Morales, G.T. Fernandez, P. Esparza, S. Gonzalez, R.C. Salvarezza, A.J. Arvia, *Corros. Sci.* 37 (2) (1995) 211.
- [17] M.B. Valcarce, M. Vázquez, S.R. de Sánchez, XIII Congreso Argentino de Fisicoquímica y Química Orgánica, Bahía Blanca, Argentina, vol. II, Asociación Argentina de Investigación Fisicoquímica, 2003, p. 215.
- [18] R.M. Souto, S. González, R.C. Salvarezza, A.J. Arvia, *Electochim. Acta* 39 (17) (1994) 2619.
- [19] M.B. Valcarce, J.P. Busalmen, S.R. de Sánchez, *Inter. Biodet. Biodeg.* 50 (2002) 61.
- [20] B.S. Kim, T. Piao, S.N. Hoier, S.M. Park, *Corros. Sci.* 37 (4) (1995) 557.
- [21] C.H. Pyum, S.M. Park, *J. Electrochem. Soc.* 133 (10) (1986) 2024.
- [22] Z. Xia, Z. Szklarska-Smialowska, *Corrosion (NACE)* 46 (1990) 85.
- [23] D.A. Jones, *Principles and Prevention of Corrosion*, Macmillan Publishing Company, New York, 1992 p. 131.
- [24] D. Wagner, A.H.L. Chamberlain, *Biodegradation* 8 (1997) 177.
- [25] M.M. Critchley, N.J. Cromar, N.C. McClure, H.J. Fallowfield, *J. Appl. Microbiol.* 94 (2003) 501.